Strong optical nonlinearities due to shallow impurities in CdS

T. Hönig*
Institut für Festkörperphysik der Technischen Universität Berlin, Hardenbergstrasse 36, D-1000 Berlin 12, Federal Republic of Germany

J. Gutowski
Institut für Experimentelle Physik, Universität Bremen, Kufsteiner Strasse, D-2800 Bremen 33, Germany

M. Nägele and I. Broser
Institut für Festkörperphysik der Technischen Universität Berlin, Hardenbergstrasse 36, D-1000 Berlin 12, Federal Republic of Germany

(Received 13 August 1991)

Broadband absorption dominates in the energy range below the free excitons in CdS, being enhanced with increasing concentration of shallow impurities. This absorption is bleached under high-excitation conditions which results in a strong induced transmission. A further increase of the excitation density yields counteracting induced absorption. The characteristic experimental data are sensitively dependent on the impurity concentration, a fact which is well known in experiments using In-doped samples. The non-linear transmission behavior can be explained by a model of neutralization of ionized impurities and interaction of the created free carriers with photonic polaritons. The experimental data can be described in a very simple three-level system. It is most important to state that a satisfactory fit to the experimental data is obtained only if acceptor–conduction-band, two-step, and two-photon transitions, as well as free-electron scattering, are all taken into account. The results of excitation-wavelength- and temperature-dependent measurements underscore this interpretation.

I. INTRODUCTION

In recent times, the optical properties of wide-band-gap- II-VI semiconductors became interesting for application in nonlinear optical devices in the visible and near-uv light energy range. CdS is one of the most prominent and best investigated materials in this field. In this compound, processes such as exciton-exciton scattering,[1–3] generation of biexcitons,[1,4,5] and electron-hole-plasma formation[1,6,7] yield a strong variation of the absorption coefficient α and the index of refraction n, and thus result in pronounced optical nonlinearities in the band-gap regime under high-excitation conditions.

However, all these mechanisms are of intrinsic nature and do not allow for a systematic variation of the characteristic data of the related nonlinearities. However, it is precisely this feature that is desirable in applications. As a consequence, it should be promising to deal with impurity-induced nonlinearities whose characteristics can be varied by changing the kind of impurities or their concentration. Dagenais and Sharfin[8,9] found the donor-bound-exciton absorption in CdS to be bleached under resonant cw excitation. The saturation intensity for this effect was determined to be about 58 W/cm^2. This bleaching of absorption, i.e., the change of α results in a corresponding variation of n, as well.

Similar results were obtained under resonant excitation of acceptor-exciton complexes in CdS by light of a pulsed laser.[10] The corresponding absorption line l_1 vanishes for excitation densities larger than 150 kW/cm.[2] This effect could be used for the realization of optical bistability due to bleaching of absorption.[10] In previous publications we reported on broadband induced transmission and absorption in the energy range between the free excitons and the green edge luminescence of the donor-acceptor-pair transitions in CdS.[11,12] This effect, which was originally observed in not intentionally doped CdS crystals of different thicknesses, was explained as a composition of the neutralization of ionized acceptors and the interaction of free carriers with photonic polarization.

However, a detailed and quantitative analysis of the processes involved could not be presented at that time. It is the purpose of this paper to discuss a suitable model in terms of a three-level system involving the valence band, the acceptor levels, and the donor conduction band. Additionally, we take into account intraband transitions within the latter bands. This is a somewhat simplified but very useful description of the real situation in these experiments. As a consequence of these model considerations, it is easy to understand that a strong enhancement of the induced transmission in the whole energy range would be observed if the crystals were doped with shallow impurities like In, I, or Na. This offers the opportunity to regulate the strength of the variation $\Delta\alpha$ of the absorption coefficient through the impurity nature and content. The suitability of these impurity-related nonlinearities for optically bistable operation is discussed in Ref. 13.

II. EXPERIMENTAL SETUP

Nonlinear transmission under high-excitation densities was investigated in single-beam as well as in pump-and-probe experiments. In the first case, a narrow-band dye laser of high intensity, pumped by an excimer laser, was used. The transmitted light was analyzed by a double grating spectrometer and a bialkali photomultiplier.

For the two-beam experiments, two separate dye lasers were synchronously pumped by the excimer laser, one being used as a broadband light source of low intensity (1–30 kW/cm,[2] integrated over the whole laser-emission wavelength range), the other as a narrow-band dye laser of high intensity simultaneously exciting the sample. If the probe pulse was delayed with respect to the pump pulse (up to 500 ns, using optical fibers), the lifetime of the nonlinear transmission effect could be determined. To resolve any long-term components of the optical nonlinearities, a pulsed narrow-band dye laser of high intensity and a cw Ar laser (488 nm) were used. The transmitted Ar laser light intensity was detected by a photodiode ($t_{rise} \approx 1$ ns) whose output signal was processed by a digitizing oscilloscope. Induced changes of the cw transmittance under pulse laser irradiation were measured in a time-resolved mode, resolution limited by the rise time of the detection system (photodiode and load resistance, 5 ns).

Experiments were performed at liquid-helium temperature (1.8 K) or in a continuous-helium-flow cryostat, where temperatures between 4.4 and 60 K could be realized.

The investigated CdS samples were platelets of different thicknesses (12 μm to 1 mm). Not intentionally doped samples contained a background impurity concentration of about 10^{15}/cm.[3] Doped crystals contained shallow In donors or shallow Na acceptors at concentrations ranging from 10^{16} up to 5×10^{18}/cm.[3] These values were roughly determined from the emission energies and features of the bound excitons, being compared to the measurements of Kukimoto *et al.*[14] and the calculations of Hanamura.[15]

III. EXPERIMENTAL RESULTS

A. Linear absorption of pure and doped CdS crystals

A halogen lamp was used to characterize the linear transmission spectrum of different samples in dependence of crystal thickness and impurity concentration. The results are shown in Figs. 1 and 2 for the polarization $\mathbf{E}\perp c$ of the transmitted light at 1.8 K. This polarization was chosen since transitions between the uppermost Γ_9 valence band and the conduction band in CdS are exclusively allowed for $\mathbf{E}\perp c$, as are the ground-state transitions of the free and bound excitons in this compound. Figure 1 presents the transmission spectra in the energy range of the bound excitons of three undoped CdS platelets with thicknesses of 12, 200, and 1000 μm, called CdS-1, -2, and -3. For the 12-μm sample CdS-1, a sharp absorption structure I_2 can be observed, which is due to the creation of a donor-bound-exciton complex (curve *a*).

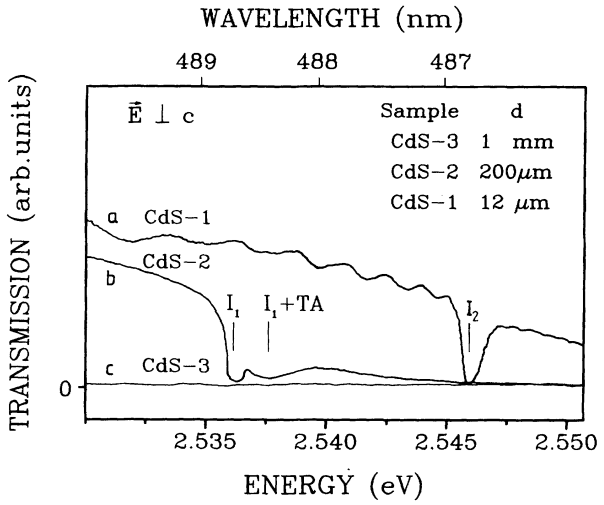

FIG. 1. Low-density transmission spectra of three CdS samples of different thicknesses, 12 μm (CdS-1), 200 μm (CdS-2), and 1000 μm (CdS-3). I_2 is the absorption of the donor-bound exciton, I_1 that of the acceptor-bound exciton, and I_1+TA its phonon replica.

To longer wavelengths, the transmittance weakly increases and Fabry-Pérot structures occur.

The 200-μm-thick crystal (curve *b*) exhibits two sharp absorption lines due to the generation of an acceptor-exciton complex without (I_1) and with additional creation of a transverse-acoustic phonon (I_1+TA). For energies below the I_1 transition, the transmittance increases over a wide wavelength range. In contrast to the case of the thin sample, the transmitted intensity is too low for detection in the vicinity of the energy of the donor-exciton transition I_2 and above.

Curve *c* is the transmission spectrum of the undoped 1000-μ-thick crystal. The transmitted light intensity was too weak for detection for wavelengths shorter than 490 nm.

The influence of different dopant material and concentration on the linear transmission spectrum of CdS is

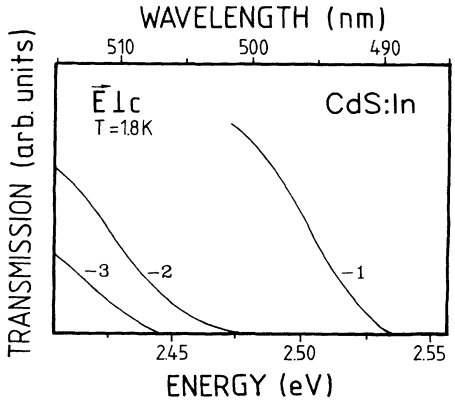

FIG. 2. Low-density transmission spectra of doped samples. Dopant concentrations are $\sim10^{17}$/cm^3 [(CdS:Na)-1, Na], $\sim5\times10^{17}$/cm^3 [(CdS:In)-2, In], and $\sim5\times10^{18}$/cm^3 [(CdS:In)-3, In].

shown in Fig. 2 for a 20-μm-thick Na-doped sample [$\sim 10^{17}/cm^3$, sample (CdS:Na)-1] and two CdS:In crystals of nearly equal thickness (700 and 800 μm) but different In concentration [5×10^{17} cm^3, (CdS:In)-2, and $5\times10^{18}/cm^3$, (CdS:In)-3]. Na is known to be an electron-acceptor and In an electron-donor material in II-VI compounds. However, when doping CdS with donors or acceptors, a large number of the opposite kind of impurities is built in as well, what is due to the strong self-compensation. Comparing the transmission spectra of samples with similar thicknesses but different impurity concentrations [see samples (CdS:In)-2 and -3], the range of rapidly increasing transmittance shifts towards longer wavelengths for increasing shallow impurity content.

B. Nonlinear absorption

1. Induced transmission

Under high-excitation conditions, strongly nonlinear behavior of the absorption coefficient in the bound-excitation region and below is observed in all undoped as well as in the doped CdS samples. In two-beam experiments, a nonlinearly increasing probe transmission signal can be obtained for growing pump intensities (see Fig. 3 for the 1000-μm-thick undoped sample). Again, a polarization $\mathbf{E}\perp c$ is chosen for the pump as well as for the probe beam due to the transition rules in CdS (see Sec. III A). A pump polarization $\mathbf{E}\parallel c$ leads to a much weaker effect without yielding additional information. It is thus only used if a reduced efficiency of the effect was desired, especially when short pump wavelengths were used (e.g., see Figs. 6–8). The bleaching of absorption is best observed on the long-wavelength side of the excitonic transitions, i.e., is mainly a bleaching of the broadband absorption mentioned above. It should further be noticed that a bleaching of the bound-exciton absorption resonances I_1 and I_2 is practically not observed in pump-and-probe experiments, which contrasts with the result of resonant single-beam transmission.[10] This is due to the fact that there is no resonant excitation of the bound-exciton transitions under observation in the two-beam experiments. Thus the number of excited bound excitons remains much smaller than in the one-beam case, staying away from bleaching.

The initial unpumped absorption coefficient being measured for energies below the bound-exciton energy (see Fig. 2) increases with growing impurity concentration which yields a more pronounced bleaching contrast when pumping is practiced. Additionally, the energy range of strong bleaching of absorption is expanded to longer wavelengths. Figure 4 shows the two-beam transmission spectra of the two CdS: In samples of different dopant concentrations [(CdS:In)-2: $\sim5\times10^{17}/cm^3$, (CdS:In)-3: $\sim5\times10^{18}/cm^3$]. The probe transmittance of the more lightly doped sample CdS:In-2 is increased by two orders of magnitude compared with the unpumped case if pumped with light of 4.5 MW/cm^2 at $\lambda_p=495$ nm. The bleaching contrast is much larger than observed for the undoped samples.

Pump-and-probe excitation spectroscopy. If the transmitted light intensity of the probe laser is detected at a fixed wavelength while the pump wavelength is varied, one obtains a kind of "excitation spectrum" of the nonlinear probe transmission. Figure 5 presents such spectra. The probe transmission is recorded for fixed spectrometer positions. The pump intensity amounts to 1.1 MW/cm^2. Induced transmission starts to be observed for pump laser wavelengths shorter than that of the donor-acceptor-pair transition at about 520 nm, smoothly increasing for decreasing pump wavelength. An edge marking the beginning of a steeper increase of the excitation efficiency is found at 513 nm, which corresponds to the onset energy of acceptor–conduction-band transitions. The spectra are directly compared with an excitation spectrum *a* of the donor-acceptor-pair (DAP) luminescence recorded on its zero-phonon band at 518.5 nm and showing a striking similarity to spectra *b*–*d*.

Sharp excitation resonances are obtained in the

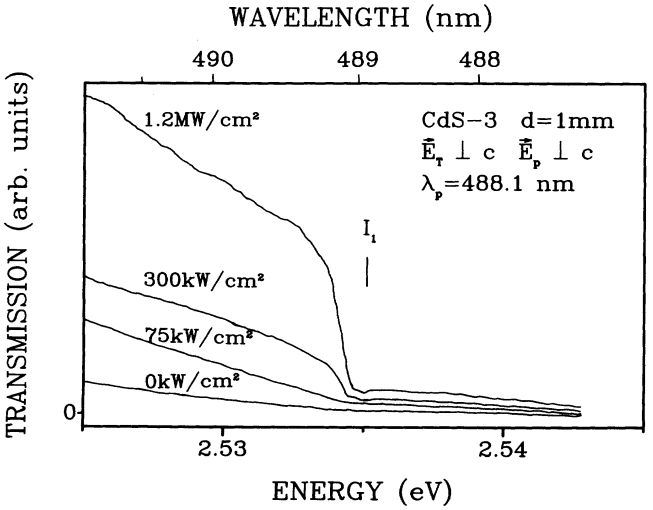

FIG. 3. Probe transmission spectra of a 100-μm-thick sample in a two-beam pump-and-probe experiment. Power density values refer to incident pump light intensity ($\lambda_p=488.1$ nm).

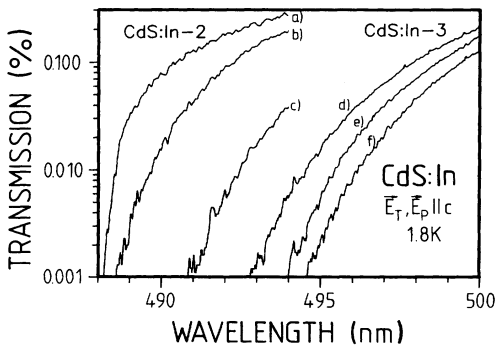

FIG. 4. Probe transmission spectra of two In-doped CdS samples for different pump light intensities. (a) 4.5 MW/cm^2; (b) pump density 1.5 MW/cm^2, $\lambda_p=495$ nm; (c) CdS:In, In concentration $\sim5\times10^{17}/cm^3$, unpumped; (d) 600 kW/cm^2; (e) pump density 300 kW/cm^2, $\lambda_p=488$ nm; (f) In concentation $\sim5\times10^{18}/cm^3$, unpumped. Efficient bleaching of absorption is obtained in both cases.

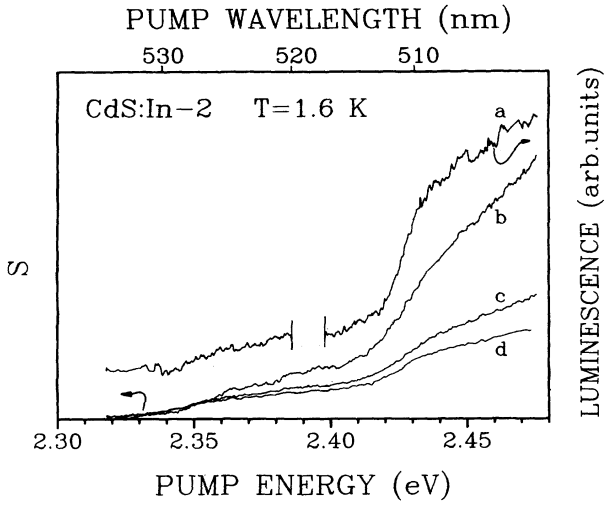

FIG. 5. Excitation spectra of the zero-phonon line 518.5 nm of the donor-acceptor-pair (DAP) luminescence (curve *a*) and of the induced transmission for fixed spectrometer positions 490 (curve *b*), 492 (curve *c*), and 497.5 (curve *d*) nm. All spectra are recorded for a pump density of 1.1 MW/cm^2 and at $T=1.6$ K, using the CdS:In sample CdS:In-2 of $\sim 5\times 10^{17}$/cm^3 In concentration. $S=(T-T_0)/T_0$, T transmission with, T_0 without pump.

bound-exciton energy range only. Figure 6 shows the excitation spectrum of the probe transmission of the 1000-μm-thick sample, being detected at 489.305 nm, just on the low-energy side of the acceptor-exciton transition I_1 which is seen as a resonance of the induced transmission, accompanied by a maximum at its phonon replica $I_1+\mathrm{TA}$ and by further maxima I_1^i known as transitions into excited electronic states of the same acceptor-exciton complex.[16–18] A roughly linear increase of the transmission is seen for pump intensities up to 400 kW/cm^2; however, a distinct saturationlike behavior is obtained at 1.6 MW/cm^2. Similar results were obtained for thinner undoped samples whereas doped samples do not exhibit such sharp excitation resonances in the bound-exciton region.

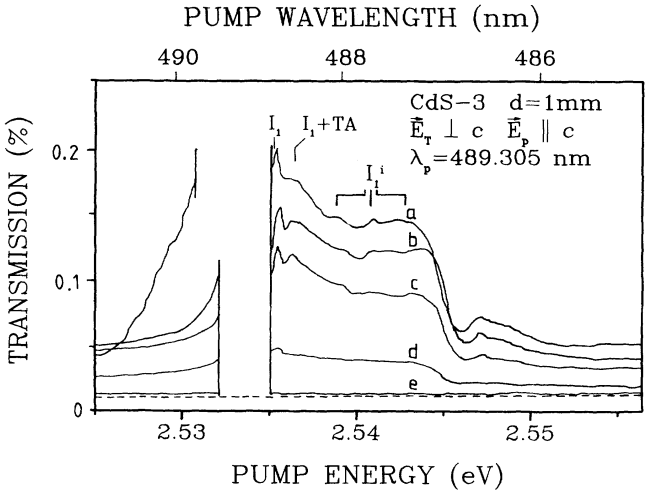

FIG. 6. Excitation spectra of the induced transmission of an undoped CdS sample of 1000 μm thickness at a recording wavelength of $\lambda_T=489.305$ nm. Pump densities 1.6 MW/cm^2 (curve *a*), 400 kW/cm,^{2} (curve *b*), 300 kW/cm^2 (curve *c*), 100 kW/cm^2 (curve *d*), and 2 kW/cm^2 (curve *e*). The laser passing the spectrometer position at λ_T is suppressed for clarity of the spectra. For explanation of the resonance, see text.

2. *Induced absorption*

For thinner undoped samples, counteracting induced absorption occurs at higher excitation densities. Figure 7 shows the development of the transmission spectra of a 200-μm-thick undoped CdS platelet under pump-and-probe conditions. For pump intensities up to 135 kW/cm^2 [shown in Fig. 7(a)], the above-described bleaching of absorption in the spectral range between the free excitons and the donor-acceptor-pair transitions (520 nm) is obtained (spectra only shown for $\lambda<491$ nm). For excitation densities higher than 135 kW/cm,^{2} induced absorption becomes dominant over the effect of bleaching [Fig. 7(b)]. This broadband increase of the absorption coefficient could be detected in the range between the band edge and wavelengths longer than 800 nm. For the highest pump densities applied (1.4 MW/cm^2), the transmission intensity on the long-wavelength side of the I_1 absorption dip falls below the unpumped transmission level.

The same effect of a combination of bleaching and induced absorption can be observed for a 20-μm-thick undoped crystal (not shown here). However, the intensity at which induced absorption becomes dominant is definitely lower. The transmission levels as function of

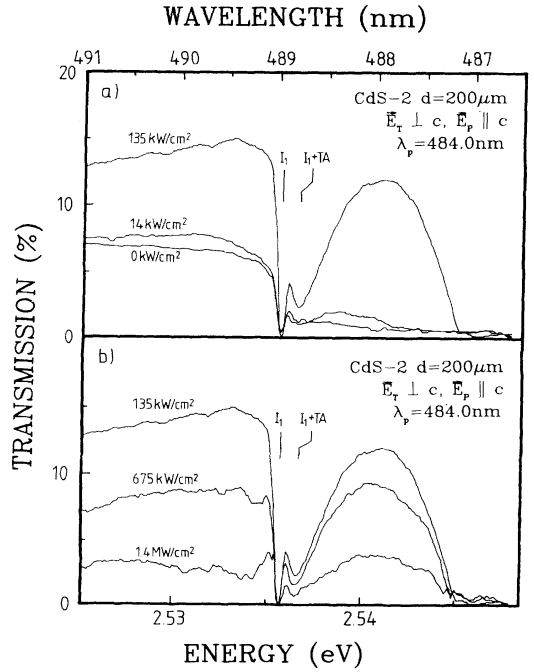

FIG. 7. Induced transmission and absorption of a 200-μm-thick, undoped CdS sample. Densities given refer to pump light intensity. Up to 135 kW/cm^2, induced transmission is observed (upper part of figure), whereas, for larger densities, induced absorption dominates (lower part, spectrum at 135 kW/cm^2 is reproduced for clarity).

the pump intensity are depicted in Fig. 12(b) for samples of very different thicknesses, being compared with model calculations (see Sec. IV B).

Excitation spectroscopy. Excitation spectra of the nonlinear probe transmission for pump intensities being sufficient to cause induced absorption were recorded for the 200-μm-thick crystal (see Fig. 8). The pump intensity was varied from 175 kW/cm^2 up to 3.5 MW/cm^2. An increasing absorption coefficient only occurs for pump laser energies larger than the energy distance between the donor and acceptor states, i.e., the donor-acceptor-pair transition energy. This corresponds to the same energy range for which, at lower pump densities, induced transmission is detected (see Sec. III B 1). For increasing excitation densities, minima occur at the spectral positions of the I_1 and I_2 transitions.

3. Temperature dependence

To gain more knowledge on the creation of induced transmission and absorption based on the impurity-related optical transmissions, it is worthwhile measuring the temperature dependence of both phenomena. In Fig. 9, the normalized differential transmission signal [DTS: $S=(T-T_0)/T_0$ with T transmission with and T_0 transmission without additional pump] of the transmitted intensity for pump densities of 200 kW/cm^2 (induced transmission) and 1.6 MW/cm^2 (induced absorption) is compared with the normalized absorption A/A_0 at the I_1 energy as a function of temperature, with S_0 and A_0 as DTS and I_1 absorption at 5 K, respectively. The wavelength position of detection was shifted with respect to the band-gap shift with increasing temperature so that a constant distance of the detection wavelength to the gap wavelength was obtained at each temperature value.

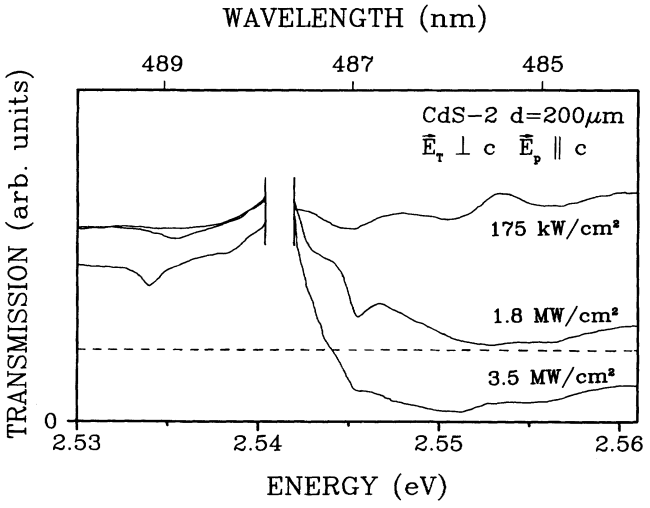

FIG. 8. Excitation spectra in the pump density range of induced absorption for the 200-μm-thick, undoped sample at a probe wavelength of $\lambda_T=487.9$ nm. Dotted line refers to the transmission level at λ_T without pump. Laser passes spectrometer position at λ_T and is suppressed for clarity. Note that for $\lambda<487.5$ nm, the absorption level for highest pump densities falls below the unpumped level.

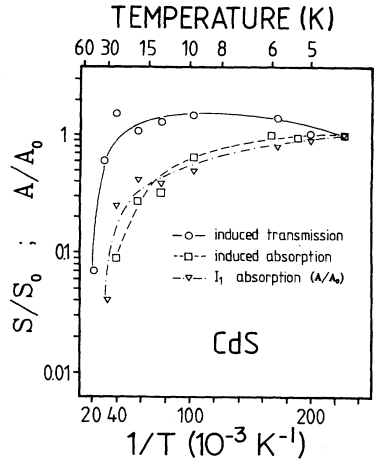

FIG. 9. Temperature dependence of induced transmission, induced absorption, and of the low-density I_1 absorption. (For pump densities, see the text.) For the first two cases, the normalized differential transmission signal S/S_0, $S=(T-T_0)/T_0$, where T is transmission in the pumped and T_0 in the unpumped case, is given; for I_1, A/A_0 as normalized absorption, with S_0 and A_0 as values at 5 K.

In agreement with previous data,[16] the I_1 absorption vanishes at about 30 K while the induced transmission ratio increases for temperatures up to 10 K. It is smoothly reduced for further elevated temperatures but still persists up to 80 K. In recent investigations, induced absorption was even observed at room temperature.[19]

4. Delay experiments

Delay experiments were performed to determine the lifetime of the strong nonlinear transmission effects. For the probe pulse delayed with respect to the incident pump pulse, the delay time Δt was determined as the time interval between the maxima of both pulses. The DTS as a function of Δt was calculated from the spectra with (transmitted probe intensity I_T) and without additional pumping (I_0). The result for induced transmission (DTS positive) is given in Fig. 10 for a 5-μm-thick slightly but unintentionally doped sample CdS-4 at a detection wavelength of $\lambda=488$ nm. Solid lines represent data obtained by the cw modulation technique for different pump intensities where the DTS as a function of time is directly visible as trace on the storage scope screen. Squares represent data obtained from a ns pump-and-probe technique with the time delay of probe to pump pulse as abscissa value. Beginning at zero delay, the DTS grows and reaches a maximum value at $\Delta t=40$ ns. The following decrease of the positive DTS is of hyperbolic nature, i.e., is described by a bimolecular recombination. The time after which the DTS is reduced to half the maximum value is about 150–200 ns. It could be shown that an increasing concentration of shallow impurities like In or Na results in a slight reduction of the decay time. However, exact data for different dopant concentrations cannot yet be obtained.

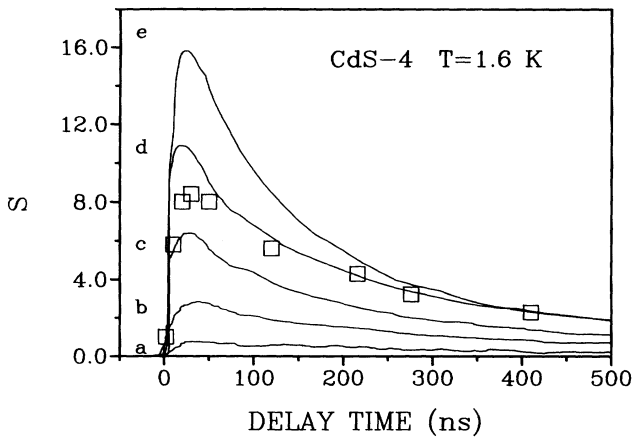

FIG. 10. Time evolution of induced transmission at $\lambda_T = 488$ nm of a 5-μm-thick, not intentionally doped CdS sample with considerably large impurity background concentration. Full lines give the development of cw modulation signal for a pump wavelength of 484 nm and densities 68 (curve *a*), 136 (curve *b*), 270 (curve *c*), 680 (curve *d*), and 1300 (curve *e*) kW/cm^2. Squares are obtained from pump-and-probe delay experiments. For details and explanation see text.

IV. DISCUSSION

A. The model

The occurrence of low-density broadband absorption on the long-wavelength side of the I_2 donor-bound-exciton line as well as its strong bleaching for higher laser intensities can be explained in a model of neutralization of ionized acceptors.

In general, not intentionally doped CdS contains a large number of shallow acceptors and donors ($\sim 10^{15}$/cm^3 to 10^{16}/cm^3). In this paper, In- and Na-doped samples (10^{16} up to 5×10^{18}/cm^3) were also investigated. Because of the *n*-type character of CdS, the concentration of donors is always larger than that of acceptors even for intentional doping with *p*-type material. Thus all acceptors are ionized as long as no external excitation takes place. An equivalent number of donors is ionized, as well.

If the samples are irradiated by light with a photon energy larger than the energy distance between the acceptor states and the conduction band, electrons are excited from the acceptor states into the conduction band, i.e., the acceptors become neutralized. This electronic transition is responsible for the broadband absorption which is, consequently, observed between the free-exciton energies and the acceptor–conduction-band transitions (513 nm at liquid-He temperatures). For longer wavelengths, the energy of the incoming photons is no longer sufficient to create free carriers. In this spectral range, the crystals become highly transmitting. If, for increasing excitation density, the number of ionized acceptors decreases, the absorption coefficient due to the neutralization of ionized acceptors becomes smaller.

As was demonstrated in Fig. 5, the excitation spectra of the impurity-related absorption are very similar to that of the donor-acceptor-pair transitions (green edge luminescence), pointing to the same excitation mechanism (see also Ref. 17). This is to be expected since the neutralization of acceptors by acceptor–conduction-band transitions, i.e., the aforementioned absorption, and the subsequent capture of the excited electrons by donors is the basis for the latter DAP transitions. The decay time being in the several hundred ns range, which was obtained from the delay measurements, results from the lifetime of the neutralized acceptors. This value is different from that given in Refs. 20 and 21, where $\tau \sim 10^{-4}$–10^{-5} s was determined from time-resolved measurements of the green edge luminescence at 77 K.

The difference may be due to the lower temperature and to a higher concentration of shallow impurities in our samples. The latter argument is supported by the observed decreasing decay time for growing impurity content.

Main evidence for a strong correlation of the shallow impurities and the broadband absorption is given by the concentration-dependent measurements. If the samples are doped with Na, which is known to be an electron-acceptor material in CdS, the absorption coefficient increases in the considered spectral range since the probability of acceptor–conduction-band transitions grows with increasing number of initial states (shallow acceptors). The same behavior was even observed if CdS was doped with an electron-donor material, e.g., indium. Because of the strong self-compensation, the concentration of shallow acceptors increases for growing In content, as well. As a further interesting result of the experiments on In-doped samples, the increase of the initial (unpumped) absorption with In concentration turned out to result in a more pronounced bleaching contrast in comparison to undoped samples (Fig. 4). This is due to the fact that the impurity-related absorption drastically increases with growing acceptor concentration, allowing for an enhanced bleaching efficiency ratio.

The effect of induced absorption, which was only detected in thinner, undoped samples under ultrahigh-excitation conditions, can be understood as interaction of photoexcited free carriers with incoming photons, i.e., photon-induced intraband transitions or scattering processes. Consequently, induced absorption was even detected at very long wavelengths like 800 nm (see Sec. III B 2). This nonlinearly increasing absorption strongly depends on the number of occupied states in the conduction band. Electrons are not only excited into the conduction band via the above-mentioned neutralization process of ionized acceptors but also by two-step processes via the resulting neutralized acceptor states, and by two-photon transitions directly from the valence into the conduction band.

As a consequence, any attempt to describe the nonlinear transmission behavior in total must consider a model involving all transitions, which are depicted in Fig. 11. Besides the excitation channels, recombination has to be taken into account. In particular, the conduction-band–acceptor and the conduction-band–valence-band recombination leads to a reduction of the free-carrier concentration which is additionally varied through electron diffusion being strongly correlated with the thickness of the samples.

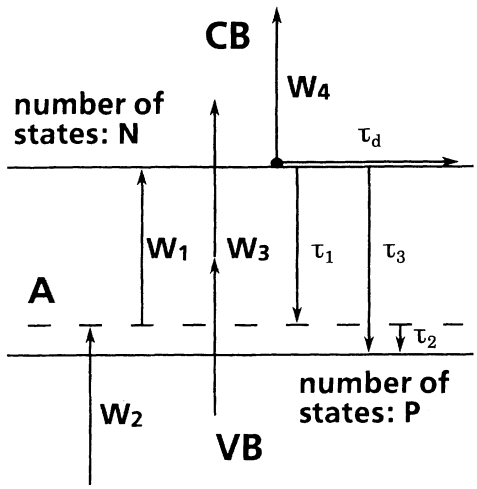

FIG. 11. Term scheme of transitions taken into account. P is the number of the relevant valence band, A of the acceptor, and N of the conduction-band states. For description of the depicted transitions, see text.

B. The model calculations

Assuming the model shown in Fig. 11 to be valid, we calculate the impurity-related absorption coefficient α_{imp} as described in Eq. (1).

$$\alpha_{\text{imp}} \sim aW_1 + PW_2 + (I/\hbar\omega)W_3 + nW_4 \ . \tag{1}$$

a and n are the numbers of electrons in the acceptor states and in the conduction band, while P represents the number of states in the valence band within a small energy range, which is given by the spectral width of the exciting laser (about 0.1 meV). The third term exhibiting a direct dependence of α on the light intensity I takes into account the two-photon transitions.

The first term aW_1 represents the acceptor–conduction-band transitions. The factor $W_1 = w_1 N$, with w_1 the transition probability, contains the number of final states, N, taken as the number of states accessible in the conduction band. The second term gives the transitions from the valence band into neutral acceptors. W_2 is not a constant and involves $A - a$ as the number of neutralized acceptors with A the total number of acceptors and a the number of electrons bound to acceptors. With w_2 as transition probability of the valence-band–acceptor transition, it reads $W_2 = w_2(A - a)$.

Donor states are omitted in this term scheme since the excitation energies are mostly chosen too small to get direct transitions from the valence band to donors, and since acceptor-donor transitions have such low probabilities that they can be neglected under the given experimental conditions.

We assume the numbers of active initial states in the valence band (P) and accessible final states in the conduction band (N) to be constant. This is justified because of the very fast relaxation time (fs) of the carriers within these bands. In contrast to that, the concentration of neutralized acceptors strongly varies with time and intensity. $(I/\hbar\omega)W_3$ gives the two-photon transitions from the valence into the conduction band with $W_3 = w_3 P$, with w_3 the two-photon transition probability, and $(I/\hbar\omega)$ the number of photons per pulse (15 ns). nW_4 describes the photon scattering at free electrons in the conduction band with probability W_4.

To determine α_{imp}, a calculation of the time-resolved number n of conduction-band electrons and of a in their dependence on the incoming intensity is necessary. Thus we establish the rate equations (2) and (3).

$$\frac{da}{dt} = W_2 P \frac{I}{\hbar\omega} + \frac{n}{\tau_1} - W_1 a \frac{I}{\hbar\omega} - \frac{a}{\tau_2} \ , \tag{2}$$

$$\frac{dn}{dt} = W_1 a \frac{I}{\hbar\omega} + W_3 \left[\frac{I}{\hbar\omega} \right]^2 - \frac{n}{\tau_1} - \frac{n}{\tau_3} - \frac{n}{\tau_d} \ . \tag{3}$$

τ_1, τ_2, and τ_3 are effective recombination "times" involving the recombination coefficients $\tau'_{1,2,3}$ and the number of final states of the decay processes. Thus they read $\tau_1 = \tau'_1 (A - a)^{-1}$, $\tau_2 = \tau'_2 (P - p)^{-1}$, $\tau_3 = \tau'_3 (P - p)^{-1}$, with p the number of electrons in the valence-band states P under consideration. The last term in Eq. (3) represents the diffusion of the free carriers in the conduction band, where the diffusion time constant τ_d is the characteristic time of carrier diffusion off the excited spot of a given diameter. For quantitative values, see below.

Finally, the equation of neutrality is necessary to solve numerically the system of the coupled differential equations (2) and (3).

The calculated values of a and n in dependence of the incoming light intensity are used to obtain α_{imp} as a function of I. The light propagation in an absorbing medium has to be calculated in the limits of the crystal thickness (d) to determine the transmitted light intensity.

$$\left. \frac{dI}{dx} \right|_{x=0}^{x=d} = -\alpha_{\text{imp}}(I) I \Big|_{x=0}^{x=d} \ . \tag{4}$$

Because of the intensity dependence of the impurity-related absorption coefficient (α_{imp}), Eq. (4) was numerically solved, as well.

In all calculations, the experimental shape of the incident light pulse was put up to enter the equations. After calculation of the numbers of free carriers (n), ionized acceptors (a), as well as of α_{imp}, a transmitted laser pulse shape $I_T(t)$ was determined. Then, $I_T(t)$ was integrated over time, allowing for a direct comparison of the theoretical and experimental results.

Calculations were performed for samples with an assumed (acceptor) impurity concentration of $a = 10^{15}/\text{cm}^3$ corresponding to not intentionally doped crystals. The number of accessible states in the valence and conduction bands was assumed to be equal for simplification, $N = P = 4 \times 10^{19}\ \text{cm}^{-3}$. According to the reasonable assumption of $\tau_1 = 10^{-9}$ s, $\tau_2 = 10^{-7}$ s, and $\tau_3 = 10^{-10}$ s, the τ' values were set as $\tau'_1 = 10^6\ \text{s cm}^{-3}$, $\tau'_2 = 10^8\ \text{s cm}^{-3}$, and $\tau'_3 = 10^5\ \text{s cm}^{-3}$ as starting values for the full incident intensity at the sample surface ($d = 0$). $W_1 = 2 \times 10^{-9}\ \text{s}^{-1}$

and $W_2=10^{-10}$ s^{-1}, expressing just a difference of the transition probabilities of both excitation processes (see Fig. 11) by a factor of 20, resulted in the best agreement of fit and experimental data whereas the two-photon absorption process with $W_3=10^{-15}$ s^{-1}cm^{-3} is weak for low light intensities but strongly increasing with I^2. W_4 had to be assumed to be $W_4=5\times10^5$ s^{-1}, giving strong intraband excitation, $\tau_d=3\times10^{-9}$ s corresponds well to carrier drift velocities like $v\approx2.5\times10^6$ cm s^{-1} (Ref. 22) off a spot of 0.1 mm radius. The thickness values entering the equations were 20, 200, and 1000 μm, which are exactly those of the three samples being systematically investigated in the pump and probe experiments (see Sec. III). The results of the calculations are shown in Fig. 12(a) presenting the transmittance $t\sim I_T/I_0$ as a function of the excitation density I_0 for the three samples (20, 200, and 1000 μm), all assumed to exhibit the same impurity concentration. The thinnest sample (20 μm) exhibits a weak bleaching of the initial absorption only and strong induced absorption for laser densities beyond 10 kW/cm^2. The 200-μm-thick crystal shows a more pronounced induced transmission lasting until excitation densities being one order of magnitude larger than for the thin crystal. Increasing absorption sets in at about 100 kW/cm^2. For the 1000-μm-thick sample, induced transmission occurs even for intensities up to 10 MW/cm^2. These calculated curves fit well to the experimental results which are presented in Fig. 12(b). The whole development of the transmittance t as a function of light intensity I_0 and thickness d at an acceptor concentration of 10^{15}/cm^3 is shown in Fig. 13 in a three-dimensional presentation. For very low intensities, the transmittance simply decreases for increasing d. Growing pump intensity I_0 results in increasing transmittance for each thickness value, however, this increase is weak for the thinnest samples due to the large initial transmission value. It is the more pronounced the thicker the sample, i.e., the lower the initial transmittance at $I_0=0$. The maximum of induced transmission shows a slight low-I_0 shift for d between 1 and 20 μm. This is due to the fact that the total number of active excited carriers yielding efficient absorption behavior remains small in very thin samples even for large carrier densities per cm.^{3} For increasing thickness, this number grows even for constant incident intensity. However, for samples thicker than 20 μm the transmission maximum drastically shifts to larger I_0, as is expected from the above-mentioned arguments. Now, the longitudinal intensity profile does not allow for a high free-carrier density through the whole sample volume for reasonable incident-intensity values. The valley of induced absorption is no longer reached even for $I_0>10^6$ W/cm^2 if samples are thicker than about 500 μm. This simulation of the experimentally found facts works so convincingly that the applicability of the model is underscored in spite of the rough transition scheme used and depicted in Fig. 11. As a consequence of the fact that the range of induced transmission shifts towards higher-excitation densities with increasing sample thickness beyond 20 μm, corresponding to the growing number of relevant impurities (acceptors), an increasing impurity concentration should lead to a development going into the same direction. As a comparison with the results obtained for the In-doped samples, calculations of the transmission for varying acceptor concentration were performed. Figure 14 shows the transmittance as a function of I_0 for two different acceptor concentration values. The theoretical results [Fig. 14(a)] do not fit the experimentally obtained development very well [Fig. 14(b)], but the model gives a qualitatively correct description of the concentration dependence. The deviations may be due to the neglect of donors as trap states as well as of the influence of the impurity concentration on the transition-probability-related factors W_1 to W_4 and τ_1 to τ_d. Concerning the time-dependent measurements depicted in Fig. 10, the hyper-

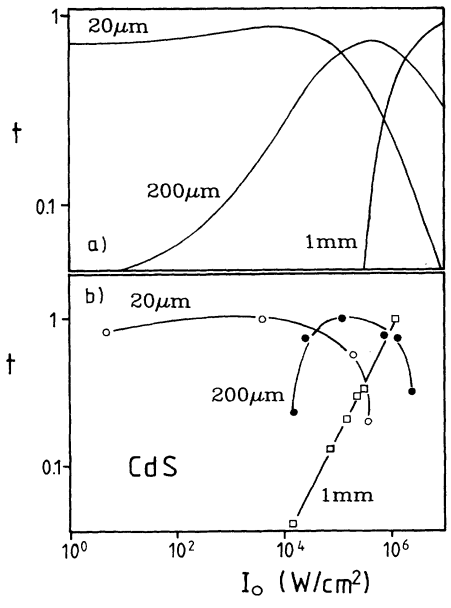

FIG. 12. Calculated (a) and measured (b) induced transmission and absorption of three samples of considerably different thickness as function of the incident pump intensity I_0. t, transmittance.

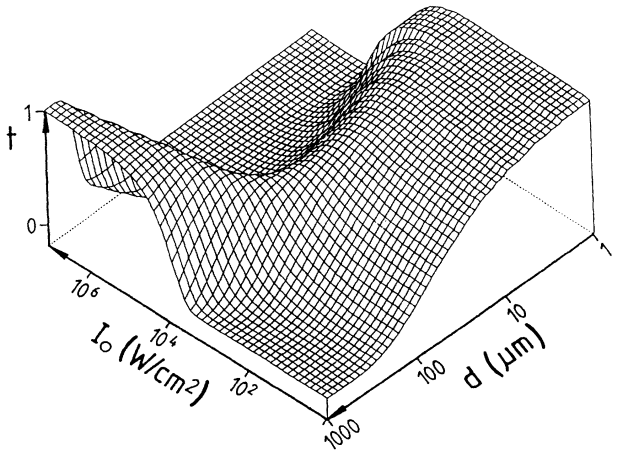

FIG. 13. Three-dimensional presentation of transmittance t as function of pump intensity I_0 and sample thickness d. For explanation, see text.

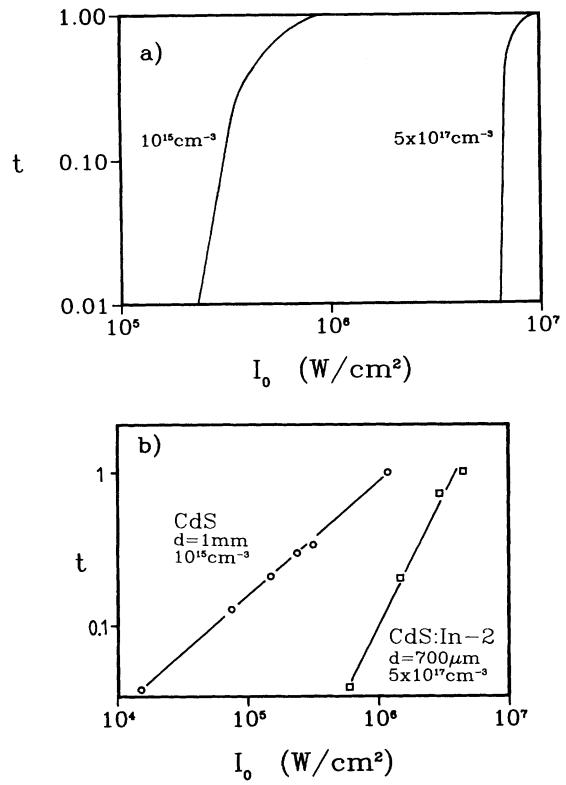

FIG. 14. Transmittance t calculated (a) and measured (b) as a function of pump intensity for two samples of different impurity concentration.

bolic decay is excellently fitted if the DTS S is assumed to be proportional to the time-dependent density of non-occupied acceptors as final states of the electron recombination from the conduction band, for which, at low densities, $n = A - a$.

$$S \sim A - a \ , \tag{5a}$$

$$d(A-a)/dt = (1/\tau_1')(A-a)^2 \ , \tag{5b}$$

with the solution

$$(A-a) = (A-a)_0/[(A-a)_0 t/\tau_1' + 1] \ , \tag{5c}$$

where $(A-a)_0$ is the number of unoccupied acceptors at $t=0$, i.e., at the time of the pump pulse peak. However, relaxation of bleaching is the long-term process only, as was seen in Fig. 10. The short-term increasing branch of the DTS can be described by taking into account the relaxation of induced absorption which is only strong for large numbers n of conduction-band electrons, i.e., for short times after the pump pulse. This complex behavior and the possibility of determining transition probabilities from the time-dependent data are planned to be extensively discussed in a future paper.[19]

V. SUMMARY AND CONCLUSIONS

In conclusion, we investigated the broadband absorption in the near-band-edge region of CdS which is strongly correlated with shallow impurities. This absorption is bleached under high-excitation conditions, and the bleaching contrast increases with increasing impurity content, i.e., increasing impurity concentration or sample thickness. For highest laser intensities, a counteracting induced absorption was observed in thinner, not intentionally doped crystals. This behavior can be explained in a model of neutralization of ionized acceptors and of the interaction of free carriers with incoming photons. Free carriers are generated by the neutralization process, two-step transitions via neutralized acceptors, and two-photon excitation. In model calculations we are able to fit our experimental data using this model. The description of the experimentally found behavior in dependence on sample thickness d and pump intensity works excellently within the model, however, this is only true if all of the above-mentioned excitation and scattering processes are taken into account. Some deviations to the experiment are obtained for the evaluation of the impurity concentration which may be overcome by considering the donors as trap states. The suitability of these nonlinearities to obtain pulse narrowing in heavily doped crystals is treated in Ref. 13; the resulting occurrence of optical bistability is critically surveyed in Ref. 23.

ACKNOWLEDGMENTS

The authors wish to thank Dr. R. Broser for supplying the crystals. This work was supported by the Deutsche Forschungsgemeinschaft (Bonn, Germany).

*Present address: FORD Germany, MC/BME-66, P.O. Box 604002, D-5000 Köln 60, Germany.

[1]C. Klingshirn and H. Haug, Phys. Rep. **70**, 315 (1981).
[2]V. G. Lyssenko and V. I. Revenko, Fiz. Tverd. Tela (Leningrad) **20**, 2144 (1978) [Sov. Phys.—Solid State **20**, 1238 (1978)].
[3]H. Kalt, V. G. Lyssenko, R. Renner, and C. Klingshirn, J. Opt. Soc. Am. B **2**, 1188 (1985).
[4]A. Kuroiwa, H. Saito, and S. Shionoya, Solid State Commun. **18**, 1107 (1976).
[5]R. Baumert, I. Broser, and K. Buschik, IEEE J. Quantum Electron. **QE - 22**, 1539 (1986).
[6]K. Bohnert, F. Fidorra, and C. Klingshirn, Z. Phys. B **57**, 263 (1984).
[7]I. Rückmann, V. May, F. Henneberger, and J. Voigt, J. Lumin. **24/25**, 593 (1981).
[8]M. Dagenais, Appl. Phys. Lett. **43**, 742 (1983).
[9]M. Dagenais and W. F. Sharfin, Opt. Eng. **25**, 219 (1986).
[10]T. Hönig and J. Gutowski, Phys. Status Solidi B **150**, 833 (1988).
[11]T. Hönig, J. Gutowski, and I. Broser, J. Cryst. Growth **86**, 576 (1988).
[12]J. Gutowski, T. Hönig, N. Presser, and I. Broser, J. Lumin. **40/41**, 433 (1988).
[13]T. Hönig, J. Gutowski, and I. Broser, in *20th International Conference on the Physics of Semiconductors, Thessaloniki (Greece) 1990*, edited by E. M. Anastassakis and J. D. Joannopoulos (World Scientific, Singapore, 1990), p. 1871.

[14]H. Kukimoto, S. Shionoya, S. Toyotomi, and K. Morigaki, J. Phys. Soc. Jpn. **28**, 110 (1970).
[15]E. Hanamura, J. Phys. Soc. Jpn. **28**, 120 (1970).
[16]R. Baumert, I. Broser, J. Gutowski, and A. Hoffmann, Phys. Rev. B **27**, 6263 (1983).
[17]T. Hönig and J. Gutowski, Phys. Status Solidi B **146**, 589 (1988).
[18]I. Broser, J. Gutowski, and R. Riedel, Solid State Commun. **49**, 445 (1984).
[19]M. Nägele, J. Gutowski, and I. Broser (unpublished).
[20]J. J. Lambe, C. C. Klick, and D. C. Dexter, Phys. Rev. **103**, 1715 (1956).
[21]I. Broser and R. Broser-Warminsky (unpublished).
[22]K. Kempf and C. Klingshirn, Solid State Commun. **49**, 23 (1984).
[23]R. Schmolke, E. Schöll, and J. Gutowski, in *5th International Conference on II-VI Compounds, Tamano (Japan)* [J. Cryst. Growth (to be published)].